Int. J. Heat Mass Transfer. Vol. 32, No. 3, pp. 541–550, 1989
Printed in Great Britain

0017–9310/89 $3.00+0.00

Inertia effects on vortex instability of a horizontal natural convection flow in a saturated porous medium

WEN-JENG CHANG and JIIN-YUH JANG†

Department of Mechanical Engineering, National Cheng-Kung University, Tainan, Taiwan 70101, Republic of China

(*Received* 28 *April* 1988 *and in final form* 8 *August* 1988)

Abstract—Inertia effects on the flow and vortex instability of a horizontal natural convection boundary flow in a saturated porous medium are examined by using the Forchheimer–extended Darcy equation of motion. In the base flow, similarity solutions are obtained for the case of the constant heat flux boundary condition. The stability analysis is based on the linear theory. The resulting eigenvalue problem, which retains the x-dependent perturbation terms, $\partial p'/\partial x$ and $\bar{u}(\partial T'/\partial x)$, is solved by the local similarity method. Effects of flow inertia are measured and examined in terms of the Forchheimer number, Fr. It is found that as Fr increases, the heat transfer rate decreases, and the susceptibility of the flow to the vortex mode of instability increases. The effect of x-dependent temperature and pressure perturbations is shown to stabilize the flow as compared with x-independent temperature and pressure perturbations.

1. INTRODUCTION

THE PROBLEMS of the vortex mode of instability in laminar free convection flow over a heated plate in a viscous fluid have been studied extensively over the past 20 years or so. The instability mechanism is due to the presence of a buoyancy force component in the direction normal to the plate surface. Linear stability analyses were performed by Hwang and Cheng [1], Haaland and Sparrow [2], Kahawita and Meroney [3] and Chen and Tzuoo [4]. In these analyses, a quasi-parallel flow model is assumed wherein the streamwise dependence of the basic flow is not neglected although the disturbances are assumed to be independent of the streamwise direction. It is shown that the nature of the stability curves change significantly when the non-parallelism of the basic flow is taken into consideration. The occurrence of vortex instability in a porous medium has been studied by Hsu *et al.* [5] for natural convection on a horizontal heated plate, by Hsu and Cheng [6] for mixed convection on a horizontal heated plate and by Hsu and Cheng [7] for natural convection on an inclined heated plate. In these analyses, non-parallel boundary layer flows are taken into consideration by the x-dependence of amplitude of the disturbances. However, the discrepancy of neutral stability curves between the non-parallel flow and the quasi-parallel flow is not shown in their papers. All of these works are based on the Darcy–Boussinesq formulation. However, at higher flow rates or in high permeability porous media, there is a departure from Darcy's law and the inertia effects not included in Darcy's model may become significant. The non-Darcy behaviour on the vortex mode of instability in a porous medium seems not to have been investigated. This has motivated the present investigation.

The Forchheimer–extended Darcy equation (Eugun model) was first used by Plumb and Huenefeld [8] to study free convection from a vertical plate embedded in a porous medium. Bejan and Poulikakos [9] reconsidered the problem and presented boundary layer solutions for the intermediate and non-Darcy flow regimes to supplement the boundary-layer analysis of Cheng and Minkowycz [10] for Darcy flow. Chen and Ho [11] considered a similar problem for the cases when the wall temperature is a power function of x. Their results indicate that the heat transfer rate decreases when the flow regime changes from Darcy to non-Darcy. Poulikakos and Bejan [12] and Prasad and Tuntomo [13] also used the Forchheimer model to study non-Darcy natural convection in a differentially heated vertical cavity. Recently, an experimental investigation of natural convection from a horizontal cylinder embedded in a porous medium was reported by Fand *et al.* [14] for both Darcy and inertia flow limits.

The purpose of this paper is to examine the inertia effects on the vortex instability of a horizontal natural convection flow in a porous medium. This is accomplished by considering the Forchheimer–extended Darcy equation of motion. In the main flow, the boundary layer approximations are invoked, and similarity solutions are obtained for the case of the constant heat flux boundary condition. The stability analysis is based on the linear theory. The disturbance quantities are assumed to be in the form of a stationary vortex roll that is periodic in the spanwise direction, with its amplitude function depending primarily in the normal coordinate and weakly on the stream-

† Author to whom correspondence should be addressed.

NOMENCLATURE

a	dimensional spanwise wave number
f	similarity stream function profile
F	dimensionless disturbance stream function amplitude
Fr	Forchheimer number, $c^{3/2}\alpha^{1/2}Ag\beta K/\nu^{5/2}$
g	gravitational acceleration
k	dimensionless wave number, $ax/(Ra_x)^{1/3}$
K	permeability
Nu_x	local Nusselt number
p'	perturbation pressure
P	pressure
Ra_x	local Rayleigh number, $\rho_\infty g\beta K(T_w - T_\infty)x/\mu\alpha$
T	temperature
T'	perturbation temperature
$\tilde{T}$	disturbance temperature amplitude
$\tilde{u}$	x-direction disturbance velocity amplitude
u, v, w	volume averaged velocity in the x-, y-, z-directions
u', v', w'	disturbance velocity in the x-, y-, z-directions
x, y, z	axial, normal, and spanwise coordinates.

Greek symbols

α	effective thermal diffusivity
β	coefficient of thermal expansion
δ_T	thermal boundary layer thickness
η	similarity variable
θ	dimensionless temperature, $(T-T_\infty)/(T_w-T_\infty)$
Θ	dimensionless disturbance temperature amplitude
μ	absolute viscosity
ν	kinematic viscosity
ρ	density
ψ	stream function
ψ'	disturbance stream function
$\tilde{\psi}$	disturbance stream function amplitude.

Subscripts

w	condition at the wall
∞	condition at the free stream.

Superscript

*	critical condition.

wise coordinate [7]. The resulting eigenvalue problem is solved using a variable step-size sixth-order Runge–Kutta integration scheme in conjunction with the Gram–Schmidt orthogonalization procedure [15] to maintain the linear independence of the eigenfunctions.

2. MATHEMATICAL FORMULATION

Before proceeding to the instability problem, consideration is given first to the basic natural convection flow along a horizontal surface, since the computation of instability criteria requires knowledge of the velocity and temperature profiles for the main flow and the solution has not been investigated before.

2.1. *The main flow*

Consider a semi-infinite, horizontal surface (T_w) embedded in a porous medium (T_∞) as shown in Fig. 1, where x represents the distance along the plate from its leading edge, and y the distance normal to the surface. The wall temperature is assumed to be a power function of x, i.e. $T_w = T_\infty + Ax^m$, where A is a constant. If we assume that: (1) properties of the fluid except for the density term that is associated with the body force are constant, and the porous media are everywhere isotropic and homogeneous, (2) the Boussinesq approximation is employed, and (3) Forchheimer's model is used for the momentum equation, then the governing equations in a Cartesian coordinate system are given by

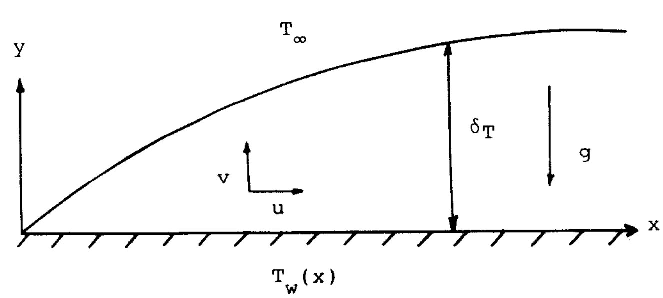

FIG. 1. Coordinate system for free convective flow in a porous medium adjacent to a horizontal heated surface.

$$\frac{\partial u}{\partial x}+\frac{\partial v}{\partial y}=0 \tag{1}$$

$$u+\frac{\rho c u^2}{\mu}=-\frac{K}{\mu}\frac{\partial p}{\partial x} \tag{2}$$

$$v+\frac{\rho c v^2}{\mu}=-\frac{K}{\mu}\left[\frac{\partial p}{\partial y}-\rho g\beta(T-T_\infty)\right] \tag{3}$$

$$u\frac{\partial T}{\partial x}+v\frac{\partial T}{\partial y}=\alpha\left(\frac{\partial^2 T}{\partial x^2}+\frac{\partial^2 T}{\partial y^2}\right) \tag{4}$$

where K is the permeability of the porous medium; β the coefficient for thermal expansion; α represents the equivalent thermal diffusivity. Note that the second term on the left-hand side of equations (2) and (3) is the inertia force in Forchheimer's model. C is the transport property related to the inertia effect. As $C = 0$, equations (2) and (3) reduce to Darcy's model. The other symbols are defined in the Nomenclature.

The pressure terms appearing in equations (2) and (3) can be eliminated through cross differentiation. By applying the boundary-layer assumptions ($\partial/\partial x \ll \partial/\partial y, v \ll u$) and introducing the stream function ψ which automatically satisfies equation (1), equations (1)–(4) become

$$\left(1+\frac{2c}{v}\frac{\partial\psi}{\partial y}\right)\frac{\partial^2\psi}{\partial y^2}=-\frac{g\beta K}{v}\frac{\partial T}{\partial x} \tag{5}$$

$$\frac{\partial\psi}{\partial y}\frac{\partial T}{\partial x}-\frac{\partial\psi}{\partial x}\frac{\partial T}{\partial y}=\alpha\frac{\partial^2 T}{\partial y^2}. \tag{6}$$

The boundary conditions for this problem are at

$$\begin{aligned}
&x>0,\quad y=0,\quad \frac{\partial\psi}{\partial x}=0;\quad T_w=T_\infty+Ax^m\\
&y\to\infty,\quad \frac{\partial\psi}{\partial y}=0;\quad T\to T_\infty\\
&x=0,\quad y>0,\quad \frac{\partial\psi}{\partial y}=0;\quad T\to T_\infty\\
&y=0,\quad \frac{\partial\psi}{\partial x}=0;\quad T\to T_\infty.
\end{aligned} \tag{7}$$

It is noted that the boundary-layer approximation leads to retention of the inertia term only in the streamwise direction.

On introducing the following transformation:

$$\eta=\frac{y}{x}Ra_x^{1/3},\quad f(\eta)=\frac{\psi}{\alpha\, Ra_x^{1/3}},\quad \theta(\eta)=\frac{T-T_\infty}{T_w-T_\infty} \tag{8}$$

where

$$Ra_x=\rho_\infty g\beta K(T_w-T_\infty)x/\mu\alpha$$

is the modified local Rayleigh number.

Equations (5) and (6) can be nondimensionalized as follows:

$$f''+\left(\frac{c^{3/2}\alpha^{1/2}Ag\beta K}{v^{5/2}}\right)^{2/3}x^{(2m-1)/3}(f'^2)' = -m\theta-\frac{m-2}{3}\eta\theta' \tag{9}$$

$$\theta''-mf'\theta+\frac{m+1}{3}f\theta'=0. \tag{10}$$

It can be seen that similarity solutions exist only if $m = 0.5$ (the constant heat flux). Then we have

$$f''+Fr^{2/3}(f'^2)'-\tfrac{1}{2}\eta\theta'+\tfrac{1}{2}\theta=0 \tag{11}$$

$$\theta''+\tfrac{1}{2}f\theta'-\tfrac{1}{2}f'\theta=0 \tag{12}$$

where

$$Fr=\frac{c^{3/2}\alpha^{1/2}Ag\beta K}{v^{5/2}}$$

is the Forchheimer number expressing the relative importance of the inertia effects. The flow is governed by Darcy's law when $Fr = 0$.

The boundary conditions are transformed as follows

$$\begin{aligned}
&\eta=0;\quad f=0,\ \theta=0\\
&\eta\to\infty;\quad f'=0,\quad \theta=0.
\end{aligned} \tag{13}$$

In terms of the dimensionless variables, it can be shown that the local Nusselt number is given by

$$Nu_x/Ra_x^{1/3}=-\theta'(0). \tag{14}$$

2.2. *The disturbance flow*

In the usual manner for stability analysis, the velocity, pressure and temperature are assumed to be the sum of a mean and fluctuating component, here designated as barred and primed quantities, respectively. We assume that the derivatives of the perturbation quantities with respect to x may not be zero. In addition, the small disturbances are functions of space variables only and this assumption proves to be useful in the study on the onset of longitudinal vortex rolls [4]. Hence, the perturbed flow can be represented as

$$\begin{aligned}
u(x,y,z)&=\bar{u}(x,y)+u'(x,y,z)\\
v(x,y,z)&=\bar{v}(x,y)+v'(x,y,z)\\
w(x,y,z)&=w'(x,y,z)\\
T(x,y,z)&=\bar{T}(x,y)+T'(x,y,z)\\
p(x,y,z)&=\bar{p}(x,y)+p'(x,y,z).
\end{aligned} \tag{15}$$

After substituting equations (15) into the governing equations for the three-dimensional convective flow in a porous medium, subtracting the parts satisfied by the base quantities, and linearizing the disturbance quantities, we arrive at the following equations for the disturbances:

$$\frac{\partial u'}{\partial x}+\frac{\partial v'}{\partial y}+\frac{\partial w'}{\partial z}=0 \tag{16}$$

$$u'+\frac{2c}{v}\bar{u}u' = -\frac{K}{\mu}\frac{\partial p'}{\partial x} \tag{17}$$

$$v'+\frac{2c}{v}\bar{v}v' = -\frac{K}{\mu}\left[\frac{\partial p'}{\partial y}-\rho g\beta T'\right] \tag{18}$$

$$w' = -\frac{K}{\mu}\frac{\partial p'}{\partial z} \tag{19}$$

$$\bar{u}\frac{\partial T'}{\partial x}+\bar{v}\frac{\partial T'}{\partial y}+u'\frac{\partial \bar{T}}{\partial x}+v'\frac{\partial \bar{T}}{\partial y} = \alpha\left(\frac{\partial^2 T'}{\partial x^2}+\frac{\partial^2 T'}{\partial y^2}+\frac{\partial^2 T'}{\partial z^2}\right). \tag{20}$$

Following the method of order-of-magnitude analysis prescribed in detail by Hsu and Cheng [7], the terms $\partial u'/\partial x$, $\partial^2 T'/\partial x^2$ in equations (16) and (20) can be neglected. The omission of $\partial u'/\partial x$ in equation (16) implies the existence of a disturbance stream function ψ' such that

$$w' = \frac{\partial \psi'}{\partial y},\quad v' = -\frac{\partial \psi'}{\partial z}. \tag{21}$$

We assume that the three-dimensional disturbances are of the form

$$(\psi', u', T') = [\tilde{\psi}(x,y), \tilde{u}(x,y), \tilde{T}(x,y)] \times \exp(iaz+\gamma(x)) \tag{22}$$

where a is the spanwise periodic wave number, and

$$\gamma(x) = \int \alpha_i(x)\,\mathrm{d}x$$

with $\alpha_i(x)$ denoting the spatial growth factor. For the lowest order approximation $\gamma(x) = \alpha_i x$ [7]. It is noted that the amplitudes of the disturbance are assumed functions of both x and y, in contrast to the parallel or quasi-parallel flow model wherein the amplitudes of the disturbance are functions of y only. Setting $\alpha_i = 0$ for neutral stability yields

$$\mathrm{i}a\tilde{u}+\frac{2\mathrm{i}ac}{v}\bar{u}\tilde{u} = \frac{\partial \tilde{\psi}}{\partial x\,\partial y} \tag{23}$$

$$\frac{\partial^2 \tilde{\psi}}{\partial y^2}-a^2\tilde{\psi}-\frac{2ca^2}{v}\bar{v}\tilde{\psi} = -\frac{\mathrm{i}aK\rho g\beta}{\mu}\tilde{T} \tag{24}$$

$$\alpha\left(\frac{\partial^2 \tilde{T}}{\partial y^2}-a^2\tilde{T}\right) = \bar{u}\frac{\partial \tilde{T}}{\partial x}+\bar{v}\frac{\partial \tilde{T}}{\partial y}+\tilde{u}\frac{\partial \bar{T}}{\partial x}-\mathrm{i}a\tilde{\psi}\frac{\partial \bar{T}}{\partial y}. \tag{25}$$

Equations (23)–(25) are solved based on the local similarity approximations [7], wherein the disturbances are assumed to have weak dependence in the streamwise direction (i.e. $\partial/\partial x \ll \partial/\partial \eta$). Letting

$$k = \frac{ax}{Ra_x^{1/3}},\quad F(\eta,x) = \frac{\tilde{\psi}}{\mathrm{i}\alpha\, Ra_x^{1/3}},$$

$$\Theta(\eta,x) = \frac{\tilde{T}}{(T_w-T_\infty)}. \tag{26}$$

We obtain the following system of equations for the local similarity approximations:

$$F''-[1-\tfrac{2}{3}B_5\, Fr^{2/3}\, Ra_x^{-2/3}]k^2F = -k\, Ra_x^{1/3}\Theta \tag{27}$$

$$\Theta''-B_2\Theta'-(k^2+\tfrac{1}{2}B_1)\Theta = B_3\frac{-\frac{1}{2}Ra_x^{-1/3}k^{-1}\eta}{(1+2Fr^{2/3}B_1)}F'' + k\, Ra_x^{1/3}B_4F \tag{28}$$

with the boundary conditions

$$F(0) = \Theta(0) = F(\infty) = \Theta(\infty) = 0 \tag{29}$$

where the primes indicate the derivative with respect to η. Equation (29) arises from the fact that the disturbances vanish at the wall and in the free stream in a porous medium. It is noted that the boundary condition $\Theta(0) = 0$ for the disturbance temperature at the wall requires that the wall temperature is truly at $T_w = T_\infty + Ax^{1/2}$. The coefficients $B_1(\eta)$–$B_5(\eta)$ in the equations can be expressed as

$$B_1 = f'$$
$$B_2 = -\tfrac{1}{2}f$$
$$B_3 = \tfrac{1}{2}\theta-\tfrac{1}{2}\eta\theta'$$
$$B_4 = \theta'$$
$$B_5 = \tfrac{3}{2}f-\tfrac{3}{2}\eta f'. \tag{30}$$

Equations (27) and (28) constitute a fourth-order system of linear ordinary differential equations for the disturbance amplitude distributions $F(\eta)$ and $\Theta(\eta)$. For fixed Fr, solutions F and Θ are eigenfunctions for the eigenvalues Ra_x and k.

One of the purposes of this paper is to examine the effect of the x-dependence temperature and pressure terms, $\partial P'/\partial x$ and $\bar{u}(\partial T'/\partial x)$ in equations (16) and (20) on the vortex instability. If we neglect these two terms, then B_1, B_2 and B_3 in equations (30) should be changed to $B_1 = 0$, $B_2 = -\frac{1}{2}f+\frac{1}{2}\eta f'$ and $B_3 = 0$, respectively.

3. NUMERICAL METHOD OF SOLUTION

In the stability calculations, the disturbance equations are solved by separately integrating two linearly independent integrals. The full equations may be written as the sum of two linearly independent solutions

$$F = F_1+EF_2$$
$$\Theta = \Theta_1+E\Theta_2. \tag{31}$$

Two independent integrals (F_i, Θ_i), with $i = 1, 2,$

may be chosen so that their asymptotic solutions are

$$F_1 = N\exp(\xi\eta_\infty), \quad \Theta_1 = \exp(\xi\eta_\infty)$$
$$F_2 = \exp(\Lambda\eta_\infty), \quad \Theta_2 = 0 \tag{32}$$

where

$$N = -k\,Ra_x^{1/3}/[\xi^2-(1-\tfrac{2}{3}B_5\,Fr^{2/3}\,Ra_x^{-1/3})k^2]$$
$$\xi = \frac{B_2-\sqrt{(B_2^2+4k^2)}}{2}$$
$$\Lambda = -[1-\tfrac{2}{3}B_5\,Fr^{2/3}\,Ra_x^{-1/3}]^{1/2}k.$$

A sixth-order Runge–Kutta, variable step size integration routine is used here to solve first the fourth-order base flow system, equations (11)–(13), and the results are stored for a fixed step size, $\Delta\eta = 0.02$, which is small enough to predict accurate linear interpolation between mesh points. Equations (27) and (28) with boundary conditions, equation (29), are then solved as follows. For specified Fr and k, Ra_x is guessed. Using equations (32) as starting values, the two integrals are integrated separately from the outer edge of the boundary layer to the wall using the sixth-order Runge–Kutta variable size integrating routine incorporated with the Gram–Schmidt orthogonalization procedure [15] to maintain the linear independence of the two eigenfunctions. The required input of the base flow to the disturbance equations is calculated, as necessary, by linear interpolation of the stored base flow. From the values of the integrals at the wall, E is determined using the boundary conditions $\Theta(0) = 0$. The second boundary condition $F(0) = 0$ is satisfied only for appropriate values of the eigenvalue Ra_x. A Taylor series expansion of the second condition provides a correction scheme for the initial guess of Ra_x. Iterations continue until the second boundary condition is sufficiently close to zero (typically $<10^{-7}$).

4. RESULTS AND DISCUSSIONS

Numerical results for the tangential velocity component, normal velocity component, and temperature profiles are presented in Figs. 2(a)–(c), respectively, for various Forchheimer numbers, Fr, in the range of 0–100 under the case of a uniform heat flux boundary condition ($m = 0.5$). It is noted that $Fr = 0$ corresponds to the Darcy flow model. It is seen that the inertia effect markedly affects the velocity and temperature fields. We observe that the tangential velocity peak $f'(0)$ and the entrainment velocity decreases and the thermal boundary layer thickness increases with increasing values of Fr.

The numerical values of $f'(0)$ and $\theta'(0)$ for selected values of Fr are tabulated in Table 1. For $Fr = 0$ which implies Darcy flow was computed to be 0.8175 as compared to 0.8186 as reported in Cheng and Chang [16]. The ratios of $\theta'(0)$ for the present case to that for the Darcy case (designated $\theta'_D(0)$) vs Fr are pre-

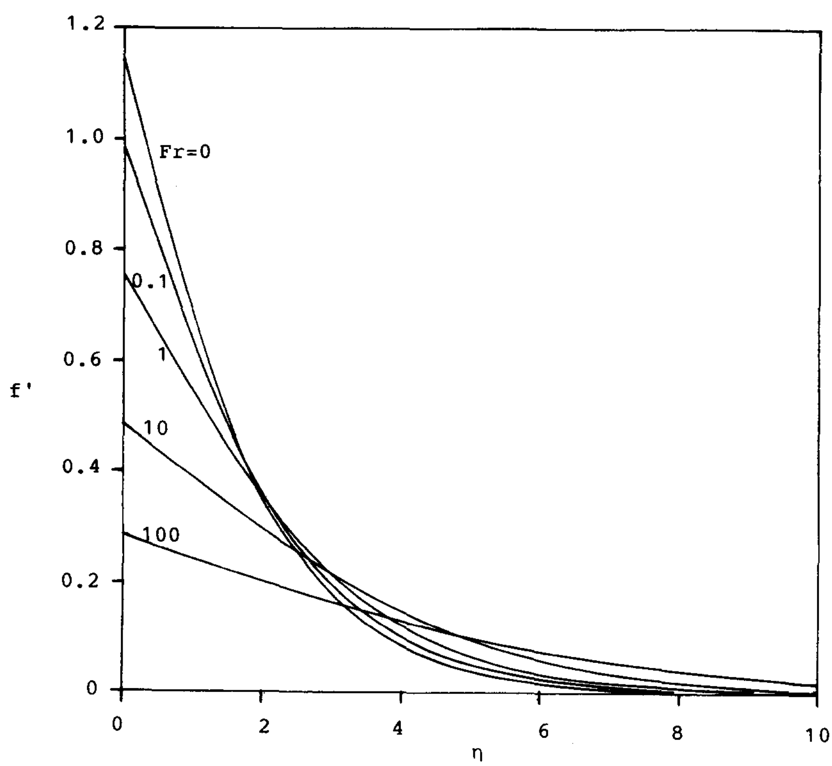

FIG. 2(a). Dimensionless tangential velocity distribution as a function of Fr.

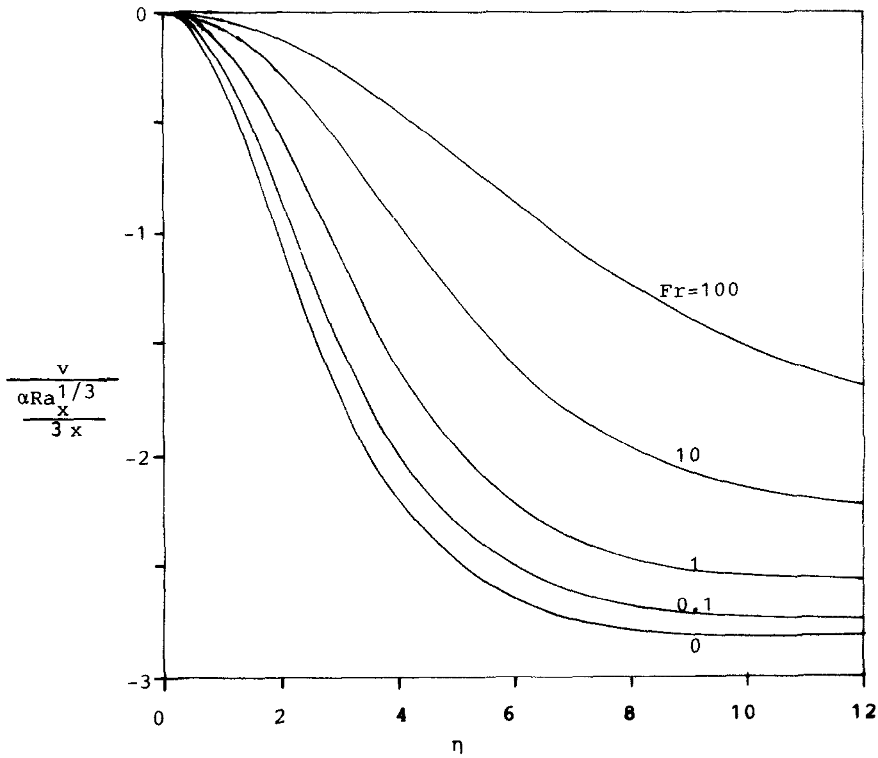

FIG. 2(b). Dimensionless normal velocity distribution as a function of *Fr*.

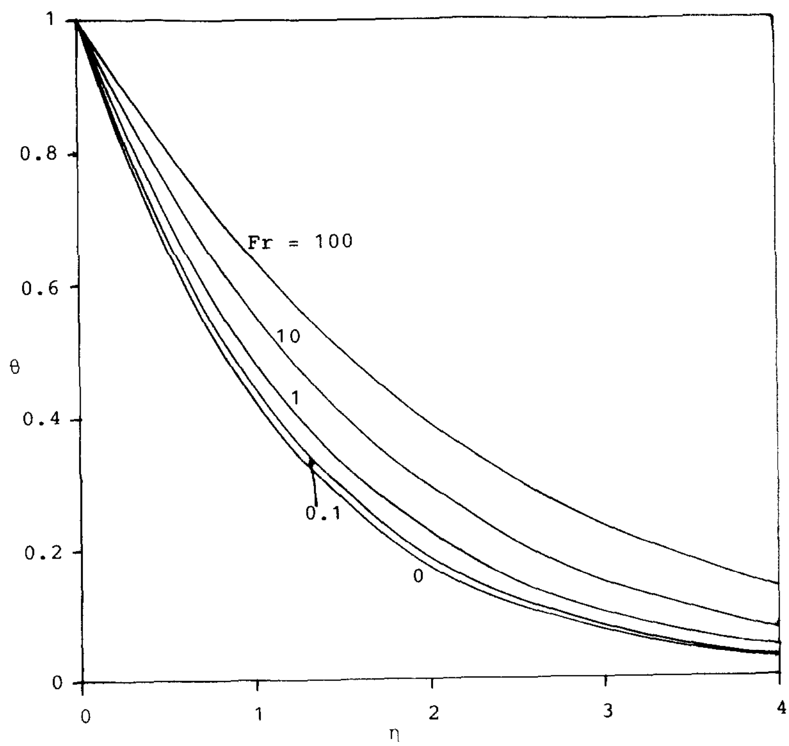

FIG. 2(c). Dimensionless temperature as a function of *Fr*.

Table 1. Dimensionless slip velocity and dimensionless temperature gradients at $\eta = 0$ for selected values of Fr

Fr	$f'(0)$	$-\theta'(0)$
0	1.140	0.8175
0.01	1.097	0.804
0.1	0.984	0.770
0.2	0.925	0.750
1.0	0.751	0.685
2.0	0.668	0.649
5.0	0.560	0.598
7.0	0.523	0.579
10.0	0.485	0.558
15.0	0.443	0.535
20.0	0.415	0.518
30.0	0.378	0.495
40.0	0.353	0.479
50.0	0.334	0.467
60.0	0.320	0.457
70.0	0.308	0.450
80.0	0.298	0.441
90.0	0.291	0.436
100.0	0.283	0.431

sented in Fig. 3. A close look at Fig. 3 indicates that, for $Fr \leqslant 0.01$, the heat transfer is within 2% of the values predicted from the Darcy flow model. However, a large error in the transport prediction may arise as Fr is increased beyond 0.1. For $Fr = 100$, the heat transfer deviates from the Darcy case by 45%.

Figure 4 shows the neutral stability curves, in terms of the flow vigour parameter Ra and the dimensionless wave number k, for selected values of Fr (0, 0.1, 0.5, 1 and 2). It is seen that as the Forchheimer number Fr increases, the neutral stability curves shift to lower Rayleigh number and lower wave number, indicating a destabilization of the flow to the vortex instability. Plotted with dashed lines in the figure for comparisons are the neutral stability curves that were obtained by neglecting the x-dependence of temperature and pressure perturbation (i.e. quasi-parallel flow model). The numerical results indicate that the effect of x-dependent disturbances is to stabilize the flow as compared with the x-independent disturbances. This is due to the presence of the x transport terms in equations (17) and (20), namely, $\partial p'/\partial x$ and $\bar{u}(\partial T'/\partial x)$, which transfer the destabilized pressure and temperature disturbances along the flow direction so that the flow becomes stabilized.

The critical Rayleigh number Ra_x^* and wave number k^*, which marks the onset of longitudinal vortices, can be found from the minima of the neutral stability curves. These critical values are listed in Table 2 for selected values of Fr and are also plotted in Figs. 5 and 6. For $Fr = 0$, the critical Rayleigh number and the wave number are computed to be 59.665 and 0.8145, respectively, as compared to 59.78 and 0.815 reported in Hsu *et al.* [5]. Both the critical Rayleigh number and critical wave number decrease as Fr (inertia coefficient) increases. The deviation of the critical Rayleigh number from that for Darcy flow is less than 10% than the Darcy model for $Fr \leqslant 0.1$. For $Fr = 2$, the deviation is up to 46%. It is also seen

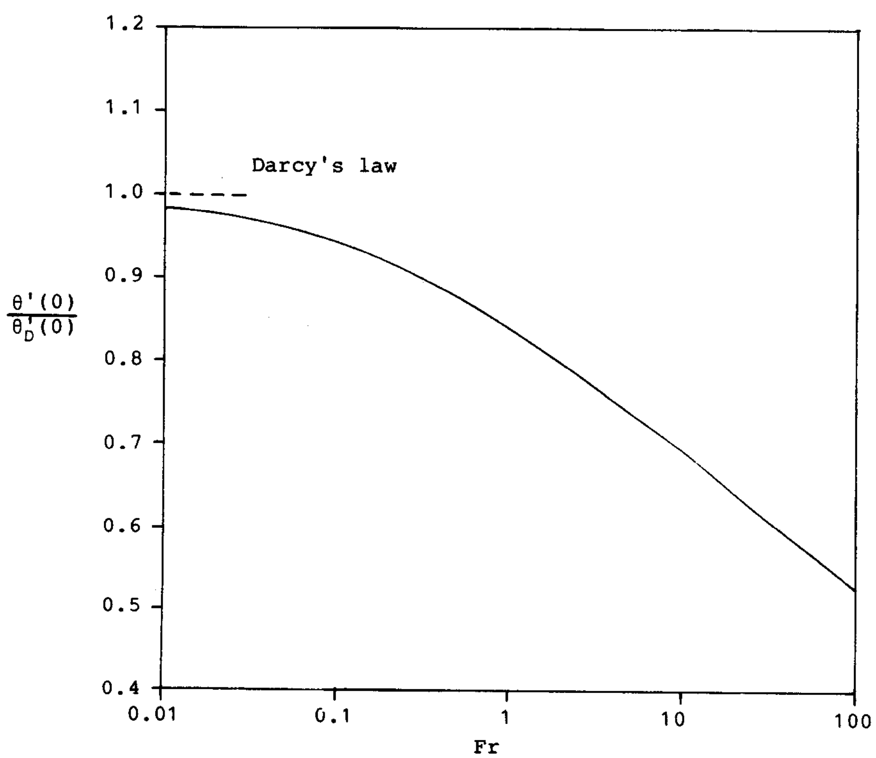

FIG. 3. The ratio of heat transfer with inertia effects to that without inertia effects as a function of Fr.

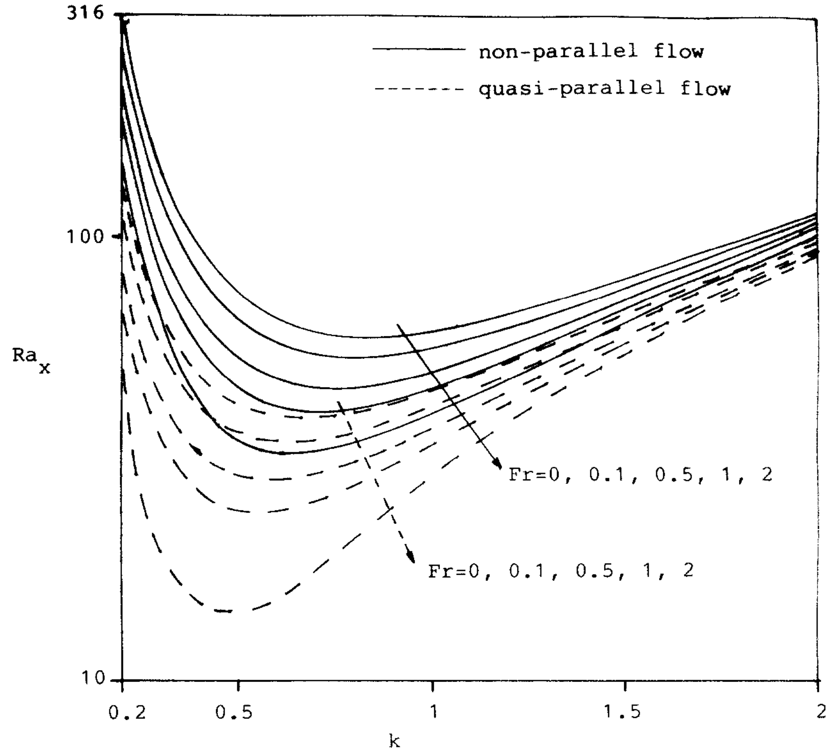

FIG. 4. Neutral stability curves for selected values of *Fr*. Solid lines denote the non-parallel flow model. Dashed lines denote the quasi-parallel flow model.

that the quasi-parallel flow model underestimates the critical Rayleigh number and critical wave number.

5. CONCLUSION

The inertia effects on the vortex instability of horizontal natural convection boundary layer flow in a saturated porous medium have been examined by a linear stability theory based on Forchheimer's model, under the assumption that the amplitudes of perturbation quantities may have non-zero streamwise derivatives. The numerical results demonstrate that the inertia effects reduce the heat transfer and destabilize the flow. It is found that the deviation of the

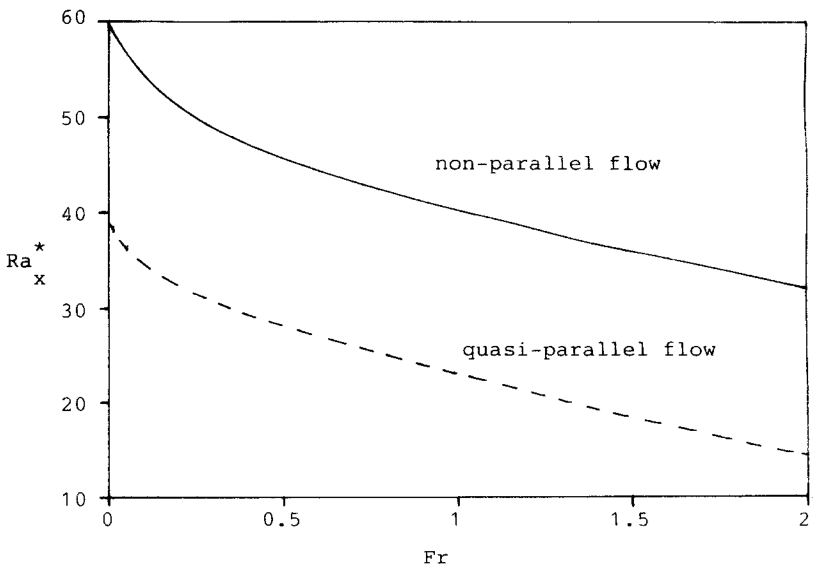

FIG. 5. Critical Rayleigh numbers as a function of *Fr*. Solid lines denote the non-parallel flow model. Dashed lines denote the quasi-parallel flow model.

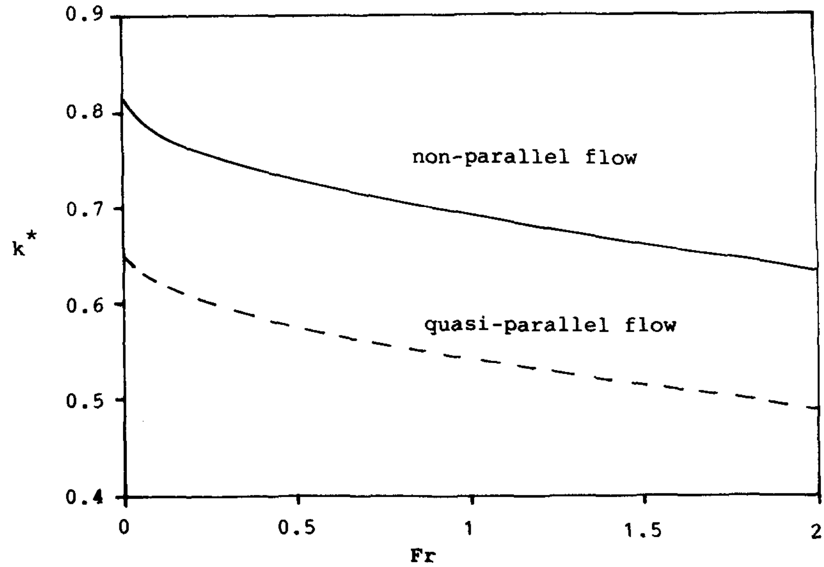

FIG. 6. Critical wave numbers as a function of *Fr*. Solid lines denote the non-parallel flow model. Dashed lines denote the quasi-parallel flow model.

Table 2. The critical Rayleigh and wave numbers vs *Fr* for non-parallel (NP) and quasi-parallel (QP) flow models

Fr	$(Ra_x^*)_{NP}$	$(Ra_x^*)_{QP}$	$(k^*)_{NP}$	$(k^*)_{QP}$
0	59.665	38.940	0.8145	0.652
0.1	53.713	34.355	0.781	0.621
0.5	45.800	28.268	0.730	0.576
1.0	40.350	23.912	0.694	0.543
2.0	32.090	14.273	0.631	0.489

critical Rayleigh number from that for the Darcy flow is less than 10% for $Fr \leqslant 0.1$. For $Fr > 0.1$, the deviation increases and inertia effects should be incorporated in the analysis. The effect of x-dependent disturbances is shown to stabilize the flow as compared with the x-independent disturbances.

REFERENCES

1. G. S. Hwang and K. C. Cheng, Thermal instability of laminar natural convection flow on inclined isothermal plates, *Can. J. Chem. Engng* **51**, 659–666 (1973).
2. S. E. Haaland and E. M. Sparrow, Vortex instability of natural convection flow on inclined surfaces, *Int. J. Heat Mass Transfer* **16**, 2355–2367 (1973).
3. R. A. Kahawita and R. N. Meroney, The vortex mode of instability in natural convection flow along inclined plate, *Int. J. Heat Mass Transfer* **17**, 541–548 (1974).
4. T. S. Chen and K. L. Tzuoo, Vortex instability of free convection flow over horizontal and inclined surfaces, *J. Heat Transfer* **104**, 637–643 (1982).
5. C. T. Hsu, P. Cheng and G. M. Homsy, Instability of free convection flow over a horizontal impermeable surface in a porous medium, *Int. J. Heat Mass Transfer* **21**, 1221–1228 (1978).
6. C. T. Hsu and P. Cheng, Vortex instability of mixed convection flow in a semi-infinite porous medium bounded by a horizontal surface, *Int. J. Heat Mass Transfer* **23**, 789–798 (1980).
7. C. T. Hsu and P. Cheng, Vortex instability in buoyancy-induced flow over inclined heated surfaces in porous media, *J. Heat Transfer* **101**, 660–665 (1979).
8. O. A. Plumb and I. C. Huenefeld, Non-Darcy natural convection from heated surfaces in saturated porous media, *Int. J. Heat Mass Transfer* **24**, 765–768 (1981).
9. A. Bejan and D. Poulikakos, The non-Darcy regime for vertical boundary layer natural convection in a porous medium, *Int. J. Heat Mass Transfer* **26**, 815–822 (1983).
10. P. Cheng and W. J. Minkowycz, Free convection about a vertical flat plate embedded in a porous medium with application to heat transfer from a dike, *Geophys. Res.* **82**, 2040–2044 (1977).
11. K. S. Chen and J. R. Ho, Effects of flow inertia on vertical natural convection in saturated porous medium, *Int. J. Heat Mass Transfer* **29**, 753–759 (1986).
12. D. Poulikakos and A. Bejan, The departure from Darcy flow in natural convection in a vertical porous layer, *Physics Fluids* **28**, 3477–3484 (1985).
13. V. Prasad and A. Tuntomo, Inertia effects on natural convection in a vertical porous cavity, *Numer. Heat Transfer* **11**, 295–320 (1987).
14. R. M. Fand, T. E. Steinberger and P. Cheng, Natural convection heat transfer from a horizontal cylinder embedded in a porous medium, *Int. J. Heat Mass Transfer* **29**, 119–133 (1986).
15. A. R. Wazzan, T. T. Okamura and H. M. O. Smith, Stability of laminar boundary layer at separation, *Physics Fluids* **190**, 2540–2545 (1967).
16. P. Cheng and I. D. Chang, Buoyancy induced flows in a saturated porous medium adjacent to impermeable horizontal surfaces, *Int. J. Heat Mass Transfer* **19**, 1267–1272 (1976).

EFFETS DE L'INERTIE SUR L'INSTABILITE TOURBILLONNAIRE D'UN ECOULEMENT HORIZONTAL DE CONVECTION NATURELLE DANS UN MILIEU POREUX SATURE

Résumé—Les effets inertiels sur l'écoulement et l'instabilité tourbillonnaire d'un écoulement horizontal de convection naturelle dans un milieu poreux saturé, sont examinés en utilisant l'équation de Forchheimer–Darcy du mouvement. Dans l'écoulement de base, on obtient des solutions de similitude dans le cas d'une condition limite de flux thermique uniforme. L'analyse de stabilité est basée sur la théorie linéaire. Le problème aux valeurs propres qui retient les termes de perturbation dépendant de x, $\partial p'/\partial x$ et $\bar{u}(\partial T'/\partial x)$, est résolu par la méthode de similitude locale. Les effets de l'inertie sont évalués et examinés en terme du nombre de Forchheimer Fr. On trouve que lorsque Fr croît, le transfert thermique diminue et las suceptibilité de l'écoulement au mode tourbillonnaire de l'instabilité augmente. L'effet des perturbations de température et de pression dépendant de x est de stabiliser l'écoulement en comparaison des perturbations de température et de pression indépendant de x.

EINFLUSS DER TRÄGHEIT AUF DIE WIRBELINSTABILITÄT IN EINER HORIZONTALEN NATÜRLICHEN KONVEKTIONSSTRÖMUNG IN EINEM GESÄTTIGTEN PORÖSEN MEDIUM

Zusammenfassung—Der Einfluß der Trägheit auf die Strömung und Wirbelinstabilität in einer horizontalen natürlichen Konvektionsströmung in einem gesättigten porösen Medium wird mit der nach Forchheimer modifizierten Darcy-Bewegungsgleichung untersucht. Für die Hauptströmung werden für den Fall einer konstanten Wärmestromdichte an der Berandung Ähnlichkeitslösungen hergeleitet. Die Stabilitätsanalyse basiert auf der linearen Theorie. Das daraus resultierende Eigenwertproblem, das die von x abhängigen Differentialterme $\partial p'/\partial x$ und $\bar{u}(\partial T'/\partial x)$ enthält, wird durch die örtliche Ähnlichkeitsmethode gelöst. Trägheitseffekte in der Strömung werden gemessen und in Form der Forchheimer-Zahl Fr betrachtet. Es zeigt sich, daß Fr ansteigt, der Wärmeübergangskoeffizient abnimmt und die Empfindlichkeit der Strömung bezüglich der Wirbelinstabilität ansteigt. Die x-abhängigen Temperatur- und Druck-Differentialterme haben einen stabilisierenden Einfluß auf die Strömung—im Vergleich zu den x-unabhängigen Temperatur- und Druckdifferentialtermen.

ВЛИЯНИЕ ИНЕРЦИОННЫХ ЭФФЕКТОВ НА ВИХРЕВУЮ НЕУСТОЙЧИВОСТЬ ГОРИЗОНТАЛЬНОГО ЕСТЕСТВЕННОКОНВЕКТИВНОГО ТЕЧЕНИЯ В НАСЫЩЕННОЙ ЖИДКОСТЬЮ ПОРИСТОЙ СРЕДЕ

Аннотация—При помощи развитого Форшхаймером уравнения движения Дарси изучается влияние инерционных эффектов на течение и вихревую неустойчивость горизонтального естественноконвективного пограничного течения в насыщенной жидкостью пористой среде. Для основного течения получены автомодельные решения в случае граничных условий с постоянной плотностью теплового потока. Анализ устойчивости течения основан на линейной теории. Полученная в результате задача на собственные значения, в которой сохраняются зависимые от x возмущения $\partial p'/\partial x$ и $\bar{u}(\partial T'/\partial x)$, решается с помощью локального преобразования подобия. Определены инерционные эффекты на основе числа форшхаймера Fr. Найдено, что с увеличением Fr снижается интенсивность теплопереноса и возрастает чувствительность течения к вихревой моде неустойчивости. Показано, что зависящие от координаты x возмущения температуры и давления стабилизируют течение по сравнению с не зависящими от x возмущениями термодинамических переменных.